International Journal of Biological Macromolecules 117 (2018) 167–178

Contents lists available at ScienceDirect

International Journal of Biological Macromolecules

journal homepage: http://www.elsevier.com/locate/ijbiomac

Antioxidant and hepatoprotective effects of purified *Rhodiola rosea* polysaccharides

Yao Xu, Huiyan Jiang, Congyong Sun, Michael Adu-Frimpong, Wenwen Deng *, Jiangnan Yu *, Ximing Xu *

Department of Pharmaceutics, School of Pharmacy, and Center for Drug/Gene Delivery and Tissue Engineering, Jiangsu University, Zhenjiang 212001, PR China

ARTICLE INFO

Article history:
Received 17 February 2018
Received in revised form 10 May 2018
Accepted 21 May 2018
Available online 24 May 2018

Keywords:
Rhodiola rosea polysaccharides
Antioxidation
Hepatoprotective

ABSTRACT

In this study, two polysaccharide fractions (RRP1: Mw = 5.5 kDa, and RRP2: Mw = 425.7 kDa) were isolated from *Rhodiola rosea* to investigate their antioxidation and hepatoprotective effects. Physicochemical analysis showed that RRP1 was composed of mannose, rhamnose, galacturonic acid, glucose, galactose and arabinose with a relative molar ratio of 0.69:0.11:0.15:1:0.51:7.5 and RRP2 was consisted of mannose, rhamnose, galacturonic acid, glucose, galactose and arabinose (relative molar ratio = 0.15:0.19:1.01:0.18:0.47:1). Periodate oxidation and Smith degradation analysis revealed that, in RRP1, part of the arabinose and glucose residues were 1 → 3,6/1 → 3/1 → 2,3/1 → 3,4/1 → 2,4/1 → 2,3,4-linked, and the mannose, rhamnose and galactose residues were 1 → 2,6/1 → 6/1 → 2/1→/1 → 4,6/1 → 4-linked. In RRP2, the rhamnose, glucose and galactose residues were linked by 1 → 3,6/1 → 3/1 → 2,3/1 → 3,4/1 → 2,4/1 → 2,3,4 linkages, and the arabinose and mannose residues were 1 → 2/1 → 6/1 → 4-linked. The methylation analysis confirmed the structure information of the two fractions. Importantly, fraction RRP1 demonstrated stronger antioxidative activities than RRP2 by scavenging DPPH, hydroxyl and superoxide anion radicals in vitro. Correspondently, RRP1 showed more significant effects than RRP2 on decreasing the levels of ALT, AST and MDA, and increasing the GSH, SOD and CAT levels in the CCl_4-treated mice. These data demonstrated that the polysaccharide RRP1 could be developed as a promising candidate for preventing and treating liver damage induced by toxic chemicals.

1. Introduction

Liver is an extremely important organ responsible for the metabolism of harmful and noxious substances from the human's metabolites and some exogenous chemicals. Thus, liver is susceptible to the toxicity from these agents hepatotoxic substances [1]. It is widely accepted that free radicals and reactive oxygen species (ROS) produced during metabolism may cause a series of pathological changes in the liver, such as lipid peroxidation chain reaction and activation of some enzymes, which lead to oxidative stress and eventually liver damage [2]. To date, supplementation of antioxidants has become a well-recognized strategy to combat ROS-mediated hepatic injury. Sayed-Ahmed et al. [3] showed that thymoquinone (TQ), a *Nigella sativa* derived-compound with strong antioxidative activities, could prevent the development of diethylnitrosamine-induced initiation of liver cancer by decreasing oxidative stress.

In recent years, natural polysaccharides have received considerable attention due to various pharmacological actions and negligible side effects [4]. *Rhodiola rosea* polysaccharide (RRP), one of the major components in the rhizome and roots of the Traditional Chinese Medicine (TCM) *Rhodiola rosea*, has shown a variety of pharmacological effects including antioxidant, antiviral, antitumor activities, etc. [5]. However, it is unknown whether RRP has hepatoprotective effects against toxic agents like CCl_4 and the structure of polysaccharide from *Rhodiola rosea* remains to be further investigated.

In the present study, two homogeneous polysaccharides named RRP1 and RRP2 were isolated from the rhizome and roots of *Rhodiola rosea*. A series of analysis, such as high-performance gel permeation chromatography (HPGPC), Fourier transform infrared (FT-IR) spectrophotometry, nuclear magnetic resonance (NMR), periodate oxidation analysis and smith degradation, methylation analysis, X-ray diffraction (XRD), scanning electron microscopy (SEM), atomic force microscope (AFM) and Congo red staining, have been performed to analyze the two polysaccharide fractions (RRP1 and RRP2). Importantly, this is the first time to investigate the hepatoprotective effect of *Rhodiola rosea* polysaccharide fractions (RRP1 and RRP2) on CCl_4-induced hepatotoxicity in mice by assessing their radical scavenging activity in vitro and hepatoprotective effect in vivo. Taken together, these findings provide the first evidence of the hepatoprotective effects of the *Rhodiola rosea* polysaccharide owing to its antioxidative action.

* Corresponding authors.
E-mail addresses: deng4956@yeah.net, (W. Deng), yjn@ujs.edu.cn, (J. Yu), xmxu@ujs.edu.cn (X. Xu).

https://doi.org/10.1016/j.ijbiomac.2018.05.168
0141-8130/

2. Material and methods

2.1. Materials

The rhizome and roots of *Rhodiola rosea* were purchased from Lin Chi Pharmacy of Zhenjiang, (Jiangsu, China) and were identified according to the identification standard of the Pharmacopoeia of the People's Republic of China. The monosaccharide standards (Arabinose, Rhamnose, D-Xylose, D-Mannose, D-Galactose, D-Glucose) and D-Galacturonic acid were procured from Aladdin Industrial Corporation while the dextran Mw standards (Dextran 670,000 Da, 270,000 Da, 80,000 Da, 25,000 Da, and 5000 Da) were purchased from Sigma-Aldrich (Shanghai, China). 2, 2-Diphenyl-1-picrylhydrazyl (DPPH) was purchased from Sigma Chemical Co. (MO, USA). Congo red and other solvents/chemicals were purchased from Sinopharm Chemical Reagent Co., Ltd. Test kits for aspartate aminotransferase (ALT), alanine aminotransferase (AST), glutathione (GSH), malonaldehyde (MDA), superoxide dismutase (SOD), catalase (CAT), and bicinchoninic acid (BCA) were purchased from Nanjing Jiancheng Bioengineering Institute (Nanjing, China).

2.2. Isolation and purification of polysaccharides

The dried rhizome and roots of *Rhodiola rosea* was extracted with distilled water with a ratio of material to solvent of 1:10 (weight/volume, w/v), at 90 °C for 2 h. Subsequently, the extracts were collected, concentrated and precipitated by adding 95% ethanol to yield a final concentration of 80% (v/v). The precipitate was kept at 4 °C overnight and deproteinized via the Savage method (chloroform: n-butyl alcohol = 5:1, repeat 5–8 times). The deproteinized solution was dialyzed in a dialysis bag (cut-off molecular weight, 3500 Da) against running water for 48 h. The crude polysaccharide, named as RRP, was obtained after lyophilization.

The lyophilized products (2 g) dissolved in double-distilled water (40 mL). The polysaccharide solution was then applied to a D315 macroreticular resin column (Φ4.0 cm × 50 cm) and eluted with distilled water for decoloration. The elution was concentrated to 30 mL and applied to a DEAE-52 column (Φ3.0 cm × 45 cm) and eluted successively with distilled water, 0.1 M, 0.3 M and 0.5 M NaCl solution (1 mL/min), respectively. The eluents were collected into centrifuge tubes (10 mL/tube) and monitored for polysaccharide content using the phenol sulfuric acid method. The elution curve was drawn with the tube number as the abscissa and the value of absorbance (at 490 nm) as the vertical coordinate. Tubes in the same elution peak were combined, concentrated, dialyzed and lyophilized. The first fraction eluted as a single peak by the distilled water was named RRP1 (Fig. 1A). The eluent from 0.1 M NaCl solution contained multiple peaks, which was further purified on a Sephadex G-100 gel column (Φ3.0 cm × 45 cm) and eluted in sequence with distilled water, 0.1 M, 0.2 M NaCl solution at a flow rate of 0.5 mL/min. The eluents were collected into centrifuge tubes (5 mL/tube). The elution curve was drawn as mentioned above. A single peak was obtained from the distilled water elution. This fraction was named RRP2 (Fig. 1B).

2.3. Characterization of RRP1 and RRP2

2.3.1. Chemical composition determination

As previously reported, the carbohydrate content was quantified using the phenol sulfuric acid colorimetric method [6]. The protein content was measured according to the Coomassie brilliant blue method [7]. The uronic acid content was determined by sulfuric acid-carbazole method [8].

2.3.2. Molecular weight analysis

The molecular weights of RRP1and RRP2 were determined by HPGPC [9], equipped with a high-performance liquid chromatography instrument (Agilent 1260), a TSKgel G4000PWxL (7.8 mm × 300 mm) and an evaporative light scattering detector (ELSD 1260). The mobile phase was 20 mM ammonium acetate at a flow rate of 0.6 mL/min. 20 μL of polysaccharide solution (1 mg/mL) was injected with the column temperature at 35 °C. The molecular weight was calculated by the calibration curve obtained using standard dextrans with a series of molecular weights (Dextran 670,000 Da, 270,000 Da, 80,000 Da, 25,000 Da and 5000 Da).

2.3.3. Monosaccharide composition analysis

Monosaccharide composition was analyzed by 1-phenyl-3-methyl-5-pyrazolone (PMP) precolumn derivation HPLC [10]. Each polysaccharide fraction (3 mg) was hydrolyzed with 1 mL of 2 mol/L trifluoroacetic acid (TFA) at 110 °C for 6 h. The excess acid was neutralized using NaOH (0.3 M). Subsequently, 500 μL of methanolic solution of 1-phenyl-3-methyl-5-pyrazolone (PMP) (0.5 mol/L), 30 μL of lactose (10 mg/mL) and 250 μL NaOH solution (0.3 mol/L) were added and mixed using a vortex mixer, and the following reaction occurred under the alkaline condition at 70 °C for 30 min. The lactose was used as an internal standard. The solution was neutralized with HCl (0.3 mol/L), and extracted with trichloromethane three times. After that, the organic phase was discarded, and the water phase was collected for HPLC. The standard monosaccharides (arabinose, rhamnose, D-xylose, D-mannose, D-galactose, D-glucose) and D-galacturonic acid were processed with the same method. The standards and polysaccharide fractions were analyzed using HPLC equipped with an Agilent Eclipse XDB-C18 column (Φ4.6 mm × 150 mm). The mobile phase consisted of three solutions: (A) a mixture of ammonium acetate solution (50 mmol/L)-0.1% formic acid; (B) a 0.1% formic acid solution; (C) acetonitrile. The gradient elution was programmed as indicated in Table S1.

2.3.4. FT-IR analysis

Each polysaccharide component (1 mg) was thoroughly mixed with the KBr powder (100 mg) and pressed into a KBr-polysaccharide pellet for the measurement by a Fourier transform infrared (FT-IR) spectrophotometer (Nicolet 170SX, Thermal Fisher Scientific, USA) in range of 400–4000 cm^{-1}.

2.3.5. NMR analysis

Two polysaccharide fractions (40 mg each) were individually dissolved in D_2O (0.5 mL) at 25 °C. The ^1H and ^{13}C NMR spectra were recorded on a Bruker AvanceII spectrometer (400 MHz) at 30 °C (30 min for ^1H NMR and 6 h for ^{13}C NMR).

2.3.6. Periodate oxidation and smith degradation analysis

The glycosidic linkage position of RRP1 and RRP2 was evaluated via the previous method [11] with slight modifications. Each sample (10 mg) was dissolved in distilled water (<25 mL) and diluted to 25 mL with potassium periodate solution (15 mM), respectively. The mixture was kept in the dark at room temperature for 8 days. A 0.1 mL of reaction solution was collected every 12 h, which was diluted to 25 mL with distilled water. The aliquots were measured using a UV spectrophotometer at a wavelength of 223 nm, until the optical density value became stable. Glycol (2 mL) was added to end the periodate oxidation. The amount of periodate consumption was calculated according to the standard curve equation ($y = 0.0086x - 0.0039$, $R^2 = 0.9994$, where x represents the concentration of potassium periodate solution and y is the absorption value at 223 nm). The oxidative solution (10 mL) was titrated with NaOH standard (0.01 M) to calculate the production content of formic acid.

The periodate product solution was dialyzed against distilled water for 48 h. The dialysis retentate was reduced with sodium borohydride ($NaBH_4$) for 24 h at 25 °C. The excess sodium borohydride was neutralized by acetic acid. The reaction solution was then dialyzed and lyophilized to obtain the resultant polyalcohol. The

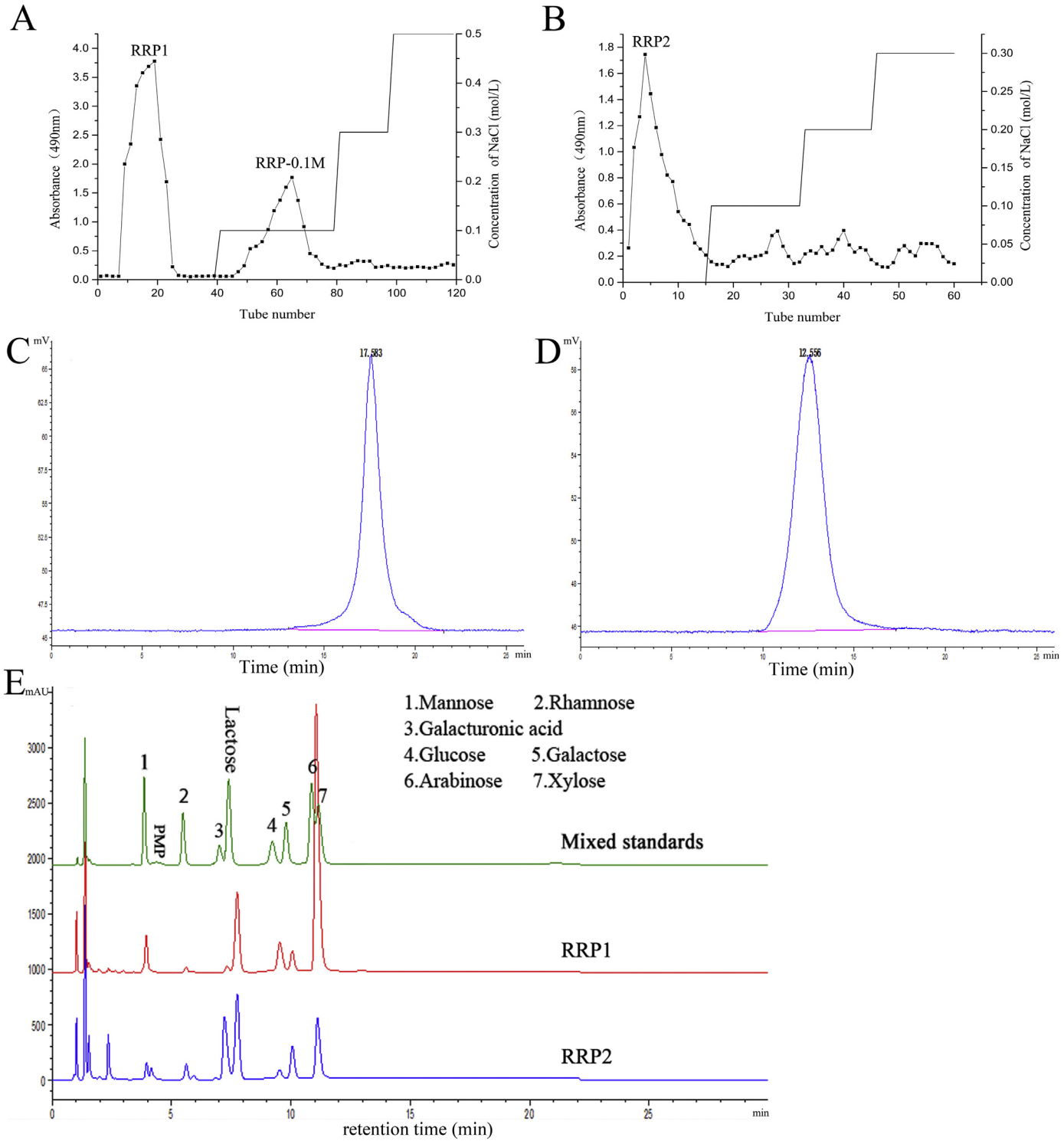

Fig. 1. (A) Elution curve of crude polysaccharide RRP on DEAE-52 chromatography column; (B) Elution curve of 0.1 M NaCl collection further purified via Sephadex G100 chromatography; (C) The HPGPC chromatogram of RRP1; (D) The HPGPC chromatogram of RRP2; (E) Chromatograms of monosaccharide compositions of the standard substance mixture, RRP1 and RRP2, respectively.

polyalcohol was hydrolyzed with 2 M TFA, acetylated, and analyzed by gas chromatography (GC) using an Agilent 7890A instrument equipped with an HP-5 capillary column (30 m × 0.32 mm × 0.25 μm) and a flame-ionization detector (FID). Nitrogen was used as the carrier gas. The temperature program was as follows: increasing from 100 °C (1 min) to 220 °C at 20 °C/min and holding at 220 °C for 11 min. The temperatures of both injector and detector were set at 250 °C.

2.3.7. Methylation analysis

Methylation analysis is one of the most important methods to study monosaccharide composition and glycosidic linkages in polysaccharides. Prior to methylation, the uronic acid of RRP1 and RRP2 was reduced twice with CMC-$NaBH_4$ [11] to obtain two corresponding neutral polysaccharides. Then these samples were then dialyzed and lyophilized for the subsequent methylation analysis according to the reported method [12]. Briefly, two dried polysaccharides were

completely dissolved in 3 mL DMSO at room temperature. The powdered dry NaOH (180 mg) was added to the solution and stirred for 1 h under the protection of N_2. CH_3I (1.5 mL) was added dropwise in dark and ice bath, and then the mixture was stirred for 30 min at room temperature. This procedure was repeated once and the reaction was terminated by adding 2 mL of distilled water. The methylated polysaccharides were extracted with dichloromethane three times and dried under N_2. The methylated product was hydrolyzed, reduced, acetylated, and analyzed by GC–MS (Agilent 7890A-5975C, USA) with a DB-5MS capillary column (30 m × 0.25 mm × 0.25 μm).

2.3.8. X-ray diffraction spectrum

The X-ray diffractograms were acquired at room temperature (20 ± 1 °C) on an X-ray diffractometer (Bruker; Type: D8 ADVANCE; Germany; Type RX: Copper). The patterns were collected in the 2θ ranges of 5–60° with 5°/min of the scan rate.

2.3.9. Congo red assay

The triple-helix structure of each purified polysaccharide fraction was determined via the Congo red method [13]. 2.0 mL of the polysaccharide solution (1 mg/mL) was mixed thoroughly with 2.0 mL of Congo red reagent (100 μM). The mixture was gradually adjusted to different NaOH concentrations (0.05, 0.1, 0.2, 0.3, 0.4, 0.5 M) by adding the NaOH solution (2 M). At each NaOH concentration, the maximum absorption wavelength of the mixture was measured with the ultraviolet-visible scanning (200–600 nm). The distilled water was used as control.

2.3.10. Scanning electron microscopy (SEM)

Scanning electron microscopy (SEM, S-3400N, Hitachi) of the samples was conducted. In brief, the polysaccharide powder was placed on the sample stage with the help of double-sided adhesive tapes and coated with the gold powder by using vacuum coating apparatus.

2.3.11. Atomic force microscope (AFM)

The topographies of samples were obtained using an atomic force microscope (AFM, MicroNaho D3000). The sample in ultrapure water at 5 μg/mL was magnetically stirred for 10 min. Subsequently, 5 μL of this solution was dropped onto freshly cleaved mica substrate and allowed to air-dry under ambient pressure, temperature and humidity. The atomic force microscope (AFM) was operated in the tapping mode at room temperature.

2.4. In vitro antioxidant activity

The scavenging activities of RRP1 and RRP2 against the DPPH, hydroxyl and superoxide anion radicals were measured.

2.4.1. DPPH radical scavenging activity

The DPPH radical scavenging activity of RRP1 and RRP2 was measured according to the reported method [14] with modest modifications. In brief, appropriate volume of each sample solution (1 mg/mL) was added to the anhydrous ethanol to reach a final volume of 1 mL. The solution was then mixed thoroughly with 2 mL of DPPH working solution (0.1 mM in anhydrous ethanol). The mixture was kept in the dark room for 30 min. The absorbance of the resultant solution was measured at 517 nm. The scavenging activity of DPPH radicals was calculated by the following equation:

$$\text{DPPH radical scavenging rate}(\%) = [1-(\text{Ai}-\text{Aj})/\text{A0}] \times 100$$

where A_0 was the absorbance of the control (deionized water instead of sample), A_i was the absorbance of the mixture of DPPH solution and the polysaccharide samples (or the positive control vitamin C, Vc), and A_j was the absorbance of background solution.

2.4.2. Hydroxyl radical scavenging activity

The hydroxyl radical scavenging activity was assessed by the method of Fenton reaction [15] with some modifications. In short, 1 mL of 1.5 mM $FeSO_4$, 1 mL of 0.75 mmol/L 1,10-phenanthroline, 1.5 mL of 0.15 mol/L sodium phosphate buffer (pH 7.4), and 1 mL of 0.1% (v/v) H_2O_2 were added to 1 mL of polysaccharide solution at various concentrations (0.06–2 mg/mL). After incubation for 30 min at 37 °C in the dark room, the absorbance of the mixture was measured at 536 nm using a UV spectrophotometer reader (Shimadzu, Japan). The scavenging activity of hydroxyl radical was calculated using the following equation:

$$\text{Hydroxyl radical scavenging rate}(\%) = [1-(\text{Ai}-\text{Aj})/\text{A0}] \times 100$$

where A_0 was the absorbance of the control (deionized water instead of sample), Ai was the absorbance of the reaction solution of polysaccharide samples (or Vc) and the hydroxyl radicals, and A_j was the absorbance of background solution.

2.4.3. Superoxide anion radical ($\bullet O_2^-$) scavenging activity

The superoxide anion radical scavenging activity assay of RRP1 and RRP2 was determined with the method described by Peng et al. with slight alteration [16]. Briefly, 0.5 mL of the polysaccharide solution with different concentrations was mixed with 5 mL of 50 mM Tris-HCl buffer (pH 8.2). Then, 0.5 mL of 5 mM pyrogallic acid was added to the mixture with a rapid shaking. After an incubation at 25 °C for 10 min, 0.1 mL of 0.1 M HCl was dripped into the mixture promptly to terminate the reaction. In this study, deionized water and Vc were used as blank and positive controls, respectively. The absorbance of the mixture was determined at 420 nm. The scavenging ability of the superoxide anion radical was calculated using the equation:

$$\text{Superoxide anion radical scavenging rate}(\%) = [1-(\text{Ai}-\text{Aj})/\text{A0}] \times 100$$

where A_0 was the absorbance of the sample blank (deionized water instead of sample), A_i was the absorbance of the tested samples, and the A_j was the absorbance of the blank reagent (Tris-HCl buffer instead of pyrogallic acid).

2.5. In vivo hepatoprotective activity

2.5.1. Animals

Male ICR mice weighing (20 ± 2) g were obtained from the Laboratory Animal Centre of Jiangsu University (Zhenjiang, China). Animals were kept under controlled conditions (room temperature 22–25 °C) and were allowed free access to drinking water and feed before experiments. All animals were humanly cared, and the experimental protocol was approved by the University Ethics Committee for the use of experimental animals and conformed to the Guide for Care and Use of Laboratory Animals.

2.5.2. Experimental design

72 mice were divided into 9 groups with 8 animals in each group. As shown in Fig. S1, the groups were named as normal control group (NC), model control group (MC), positive control group (PC), and six sample groups in which the mice were treated intragastrically with RRP1 (200, 300 and 400 mg/kg bodyweight) and RRP2 (200, 300 and 400 mg/kg bodyweight), respectively. Mice in the positive control group received silybin (100 mg/kg/d) by intragastric administration. Normal control group and model control group were administered with the same volume of distilled water in the same way. All the groups were administered once a day for 7 consecutive days. Five hours after the final administration, the mice in NC group were injected intraperitoneally with olive oil 10 mL/kg, while animals in other groups were intraperitoneally injected 10 mL/kg body weight of 2% CCl_4. All the mice

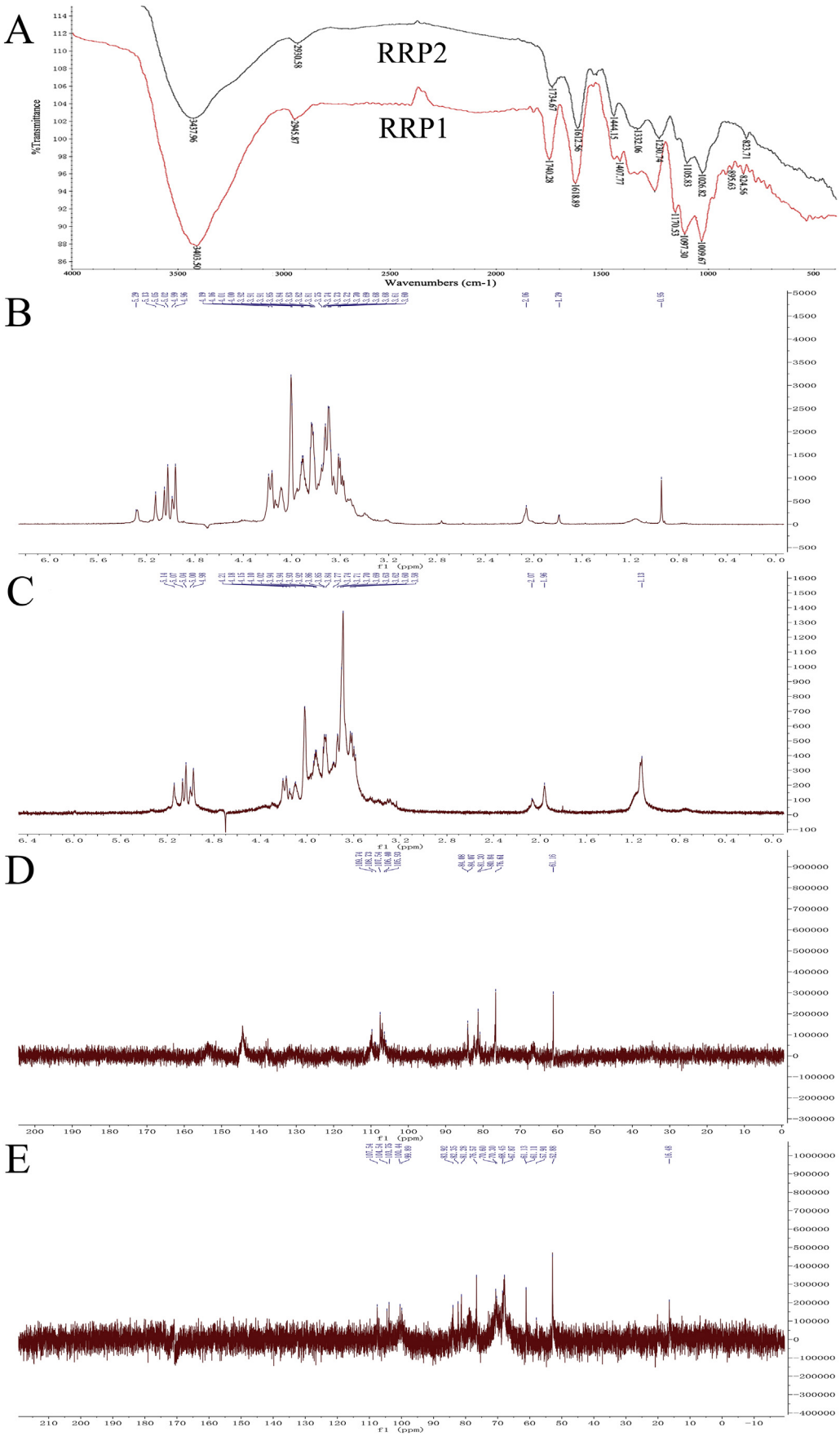

Fig. 2. Spectra analysis. (A) FTIR spectrum of RRP1 and RRP2; (B–C) ^{1}H NMR spectra of RRP1 (B) and RRP2 (C) in D_2O; (D–E) ^{13}C NMR spectra of RRP1 (D) and RRP2 (E) in D_2O.

Table 1
Periodate oxidation and glycosidic linkages position of RRP1 and RRP2.

Samples	HIO_4 consumption/mol hexose	HCOOH production/mol hexose	1 → 6 or 1 → (%)	1 → 3 (%)	1 → 2 or 1 → 4 (%)
RRP1	1.270	0.506	50.63	23.47	25.9
RRP2	1.070	0.235	23.5	16.5	60.0

were then fasted, but allowed free access to water. After 12 h, the animals were anesthetized and blood samples were collected for determination of the serum biochemical indices alongside antioxidative markers using liver homogenate; meanwhile, the histopathological change in liver was also observed.

2.5.3. Serum biochemical indexes assay

The blood samples were collected by removalling eyeballs. After that, the mice were sacrificed by cervical dislocation. The blood samples were centrifuged to separate the serum. The contents of ALT and AST in serum were determined with the kits (Nanjing Jiancheng Bioengineering Institute, Nanjing, China).

2.5.4. Liver homogenate biochemical indices assay

The liver tissue samples (0.5 g) were added into the physiological saline and pounded to pieces to obtain the tissue homogenate. After centrifugation at 3500 rpm for 15 min at 4 °C, the supernatant was collected for determination of MDA, GSH, CAT and SOD levels according to the kit instructions. The protein content of the liver homogenate was determined using BCA test kits.

2.5.5. Histopathological observation of liver

The liver tissues from the same location were taken after sacrificing the mice and washed twice with saline to remove the residual blood. Then the hepatic tissues were fixed in 4% paraformaldehyde at 4 °C for 24 h and embedded with paraffin and. 5-μm-thick slices (leica-RM2235, Wetzlar, Germany) were prepared and stained with hematoxylin and eosin (H&E; Beyotime Institute of Biology, China). The stained slices were observed using a Nikon Eclipse 90i microscope at 200× magnification.

2.6. Statistical analysis

Data were expressed as the mean ± standard deviation (S.D.). Data in all the bioassays were statistically evaluated using one-way ANOVA variance followed by Tukey's post-hoc test and $P < 0.05$ was considered to be statistically significant. Data were analyzed using Statistical Package for Social Sciences (SPSS), version 19.0 (Chicago, IL, USA).

3. Results and discussion

3.1. Isolation and purification of the Rhodiola rosea polysaccharide fractions RRP1 and RRP2

In this study, the crude polysaccharide was obtained from rhizome and roots of *Rhodiola rosea* by hot water, followed by deproteinization and decoloration. The deproteinization rate via Savage method was about 81.07 ± 1.86%. The total yield of crude polysaccharide (RRP) was 3.8% of the dried material. The RRP was then purified by DEAE-52 chromatographic column, resulting in two main peaks: RRP1 (Fig. 1A, the fraction eluted by the distilled water), and RRP2 (Fig. 1B, the fraction eluted by 0.1 M NaCl solution, which was further subjected to a Sephadex G-100 gel column and eluted by the distilled water).

According to the results of phenol sulfuric acid colorimetric method, the total carbohydrate content of RRP1 and RRP2 were (89.31 ± 1.18) % and (80.19 ± 1.68) %, respectively. The results of Coomassie brilliant blue assay showed that the protein content of RRP1 and RRP2 were (4.97 ± 0.54) % and (2.12 ± 0.37) %, respectively. The results of sulfuric acid-carbazole analysis demonstrated that RRP1 and RRP2 contained (0.90 ± 0.21) % and (14.26 ± 0.59) % of uronic acids, respectively.

3.2. Structural analysis of RRP1 and RRP2

Both RRP1 and RRP2 were recorded as a single, symmetrical chromatographic peak by HPGPC (Fig. 1C and D). The average molecular weights of RRP1 and RRP2 were estimated as 5.5 kDa and 425.7 kDa, respectively.

The monosaccharide composition of RRP1 and RRP2 was analyzed by comparing the retention time against standards using PMP-HPLC. As shown in Fig. 1E, HPLC analysis suggested that RRP1 was composed of mannose, rhamnose, galacturonic acid, glucose, galactose and arabinose with a molar ratio of 0.69:0.11:0.15:1:0.51:7.5, and the RRP2 fraction contained mannose, rhamnose, galacturonic acid, glucose, galactose and arabinose with a molar ratio of 0.15:0.19:1.01:0.18:0.47:1.

FT-IR spectroscopy was used to characterize and identify the organic functional groups in RRP1 and RRP2 [17], as depicted in Fig.2A. The strong and broad bands at 3403 cm^{-1} and 3437 cm^{-1} of RRP1 and RRP2, respectively, correspond to the O—H stretching vibrations. The weak peaks at 2945 cm^{-1} (RRP1) and 2930 cm^{-1} (RRP2) depicted C—H stretching vibrations, and the peaks at 1407 cm^{-1} (RRP1) and 1440 cm^{-1} (RRP2) indicated C—H bending vibrations. Meanwhile, the absorption bands at 1618 cm^{-1} (RRP1) and 1612 cm^{-1} (RRP2) represented C═O asymmetric stretching vibrations. The characteristic bands at 1020–1100 cm^{-1} indicated the stretching vibrations of pyranose ring [18]. Moreover, the two fractions showed weak characteristic peaks at 1741 cm^{-1} (RRP1) and 1734 cm^{-1} (RRP2), indicating the presence of uronic acids in both RRP1 and RRP2 [19]. Absorption at 824 cm^{-1} and 895 cm^{-1} showed RRP1 possessed both α-type and β-type configurations, while signals at 823 cm^{-1} depicted the existence of α-type glycosidic linkage in RRP2 [20].

Table 2
Methylation analysis by the GC–MS of *Rhodiola rosea* polysaccharides.

	RT (min)	PMAA	Linkage pattern	Molar ratio (%)
RRP1	11.703	3,4,6-Me_3-Man	1,2-linked-Man*p*	12.37
	13.213	4,6-Me_2-Arab	1,2,3-linked-Ara*p*	15.85
	14.084	2,3-Me_2-Gal	1,4,6-linked-Gal*p*	11.47
	14.240	3,4,6-Me_3-Rha	1,2-linked-Rha*p*	6.24
	14.678	2,4,6-Me_3-Glc	1,3-linked-Glc*p*	5.28
	15.696	2,3,4,6-Me_4-Man	T-Man*p*	5.51
	16.543	6-Me-Glc	1,2,3,4-linked-Glc*p*	11.86
	17.624	6-Me-Ara	1,2,3,4-linked-Ara*p*	27.37
	17.736	3,4,6-Me_3-Gal	1,2-linked-Gal*p*	4.05
RRP2	11.703	3,4,6-Me_3-Man	1,2-linked-Man*p*	19.02
	12.823	2,3,4,6-Me_4-Glc	T-Glc*p*	2.23
	13.217	3,4,6-Me_3-Arab	1,2-linked-Ara*p*	29.86
	14.084	2,3-Me_2-Gal	1,4,6-linked-Gal*p*	14.05
	14.240	3,4,6-Me_3-Rha	1,2-linked-Rha*p*	5.31
	14.615	6-Me-Glc	1,2,3,4-linked-Glc*p*	7.60
	14.678	2,3,6-Me_3-Glc	1,4-linked-Glc*p*	2.32
	15.788	2,3,4,6-Me_4-Arab	T-Ara*p*	3.38
	16.538	3,4,6-Me_3-Arab	1,2-linked-Ara*p*	8.46
	17.823	6-Me-Gal	1,2,3,4-linked-Gal*p*	7.77

The ^{1}H NMR spectrum of RRP1 (Fig. 2B) showed six peaks at δ 5.29, 5.13, 5.05, 5.02, 4.99 and 4.96 ppm in the anomeric region, indicating the existence of both α-type and β-type configurations [21]. The ^{1}H NMR spectrum of the RRP2 (Fig. 2C) depicted that another batch of peaks at δ 5.14, 5.07, 5.04, 5.00 and 4.98 ppm, indicating that these glucosyl residues were of α-type configuration, in line with the analysis of FT-IR spectrum. In addition, the ^{13}C NMR spectrum of RRP1 showed five signals at δ 105–109 ppm (Fig. 2D), which could be attributed to the anomeric carbon atoms of α-Man*p*, α-Rha*p*, α-Gal*p*, α-Ara*p* and β-Glc*p*, respectively [22]. In the ^{13}C NMR spectrum of RRP2, there were five anomeric peaks at δ 107.5, 104.5, 103.7, 100.4, and 99.8 ppm (Fig. 2E), which could be attributed to the presence of mannose, rhamnose, glucose, galactose and arabinose, respectively, in RRP2 [23].

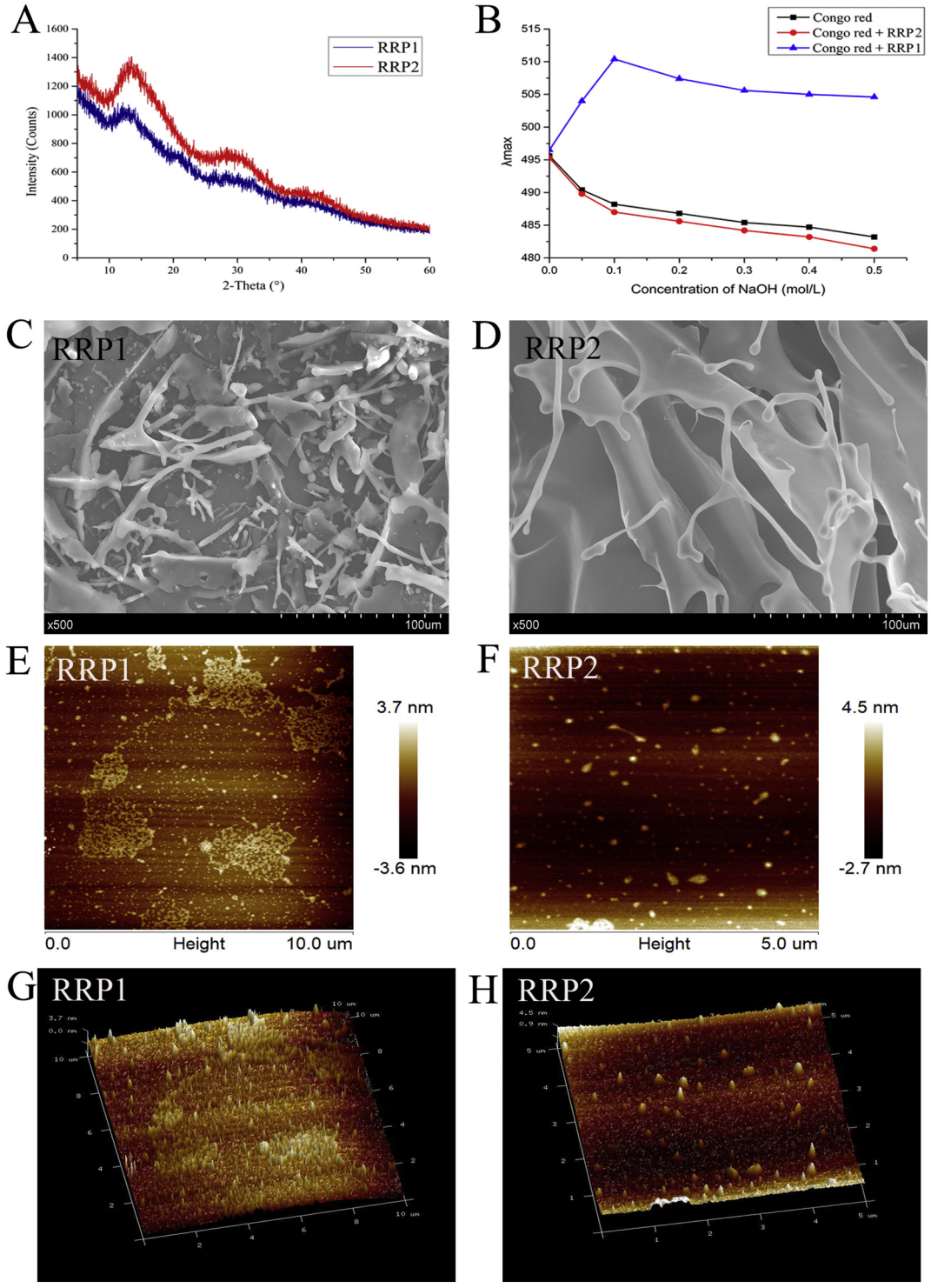

Fig. 3. Conformation and morphology analysis. (A) XRD of RRP1 (blue) and RRP2 (red); (B)The maximum absorption wavelengths of Congo red, Congo red + RRP1 and Congo red + RRP2 at various concentrations (0–0.5 mol/L) of NaOH solution; (C–D) Scanning electron microscopy (500×) of RRP1 (C) and RRP2 (D); (E-H) Atomic force microscopy planar (E for RRP1 and F for RRP2) and cubic (G for RRP1 and H for RRP2) images.

3.2.1. Periodate oxidation and smith degradation analysis

The glycosidic linkage position of the two fractions (RRP1 and RRP2) was examined via periodate oxidation method. As shown in Table 1, RRP1 consumed 1.270 mol periodic acid and produced 0.506 mol formic acid according to each mole of anhydroglucose unit. Therefore, the RRP1 were composed of 1 → 6 or 1 → (50.63%), 1 → 2 or 1 → 4 (25.9%) and 1 → 3 (23.47%) glycosidic linkages. Similarly, RRP2 contained 1 → 6 or 1 → (23.5%), 1 → 2 or 1 → 4 (60.0%) and 1 → 3 glycosidic linkages (16.5%). These findings showed that RRP1 contained a higher ratio of non-reducing glycosidic linkages (1 → 3 glycosidic linkages) as compared to RRP2.

After the oxidized products of RRP1 and RRP2 were reduced, hydrolyzed, and analyzed by GC. Four compounds of RRP1were detected include glycerin, erythritol, arabinose and glucose (Fig. S2). The presence of arabinose and glucose suggests that at least part of the arabinose and glucose residues were 1 → 3,6/1 → 3/1 → 2,3/1 → 3,4/1 → 2,4/1 → 2,3,4-linked [24]. Furthermore, mannose, rhamnose and galactose residues were absent, and massive glycerin and erythritol were produced. This result demonstrated that these three glycoside residues were 1 → 2,6/1 → 6/1 → 2/1→/1 → 4,6/1 → 4-linked in RRP1. Similarly, the presence of rhamnose, glucose and galactose in RRP2 revealed some residues of these glycoside residues were linked by 1 → 3,6/1 → 3/1 → 2,3/1 → 3,4/1 → 2,4/1 → 2,3,4 glycosidic linkages (Fig. S2). Meanwhile, a small amount of glycerin and erythritol generated during oxidation indicated that arabinose and mannose residues were 1 → 2/1 → 6/1 → 4-linked in RRP2 [25].

3.2.2. Methylation analysis

The fully methylated RRP1 and RRP2 were hydrolyzed and analyzed by GC–MS. The identification and proportions of the methylated alditol acetates of RRP1 and RRP2 were listed in Table 2. The results demonstrated that RRP1 contained 1, 2-Man*p* (12.37%), 1, 2, 3-Ara*p* (15.85%), 1, 4, 6-Gal*p* (11.47%), 1, 2-Rha*p* (6.24%), 1, 3-Glc*p* (5.28%), Terminal (T)-Man*p* (5.51%), 1, 2, 3, 4-Glc*p* (11.86%), 1,2,3,4-Ara*p* (27.37%) and 1, 2-Gal*p* (4.05%). The RRP2 was composed of 1, 2-linked-Man*p* (19.02%), T-Glc*p* (2.23%), 1, 2-linked-Ara*p* (29.86%), 1, 4, 6-linked-Gal*p* (14.05%), 1, 2-linked-Rha*p* (5.31%), 1, 2, 3, 4-linked-Glc*p* (7.60%), 1, 4-linked-Glc*p* (2.32%), T-Ara*p* (3.38%), 1, 2-linked-Ara*p* (8.46%) and 1, 2, 3, 4-linked-Gal*p* (7.77%).

3.2.3. X-ray diffraction (XRD) spectrum

XRD is a widely used technique for the analysis of the crystalline structure of polysaccharides [26]. In this study, the XRD patterns recorded for RRP1 and RRP2 were between 5° and 60° (Fig. 3A). The X-ray diffraction curve of RRP1 contained only one "bun-shaped" peak at the angel (2θ) about 13° and no sharp peaks, indicating that RRP1 was semi-crystalline substance [27]. Compared with RRP1, RRP2 showed a clearer diffraction peak when 2θ was about 14°, as well as a "bun-

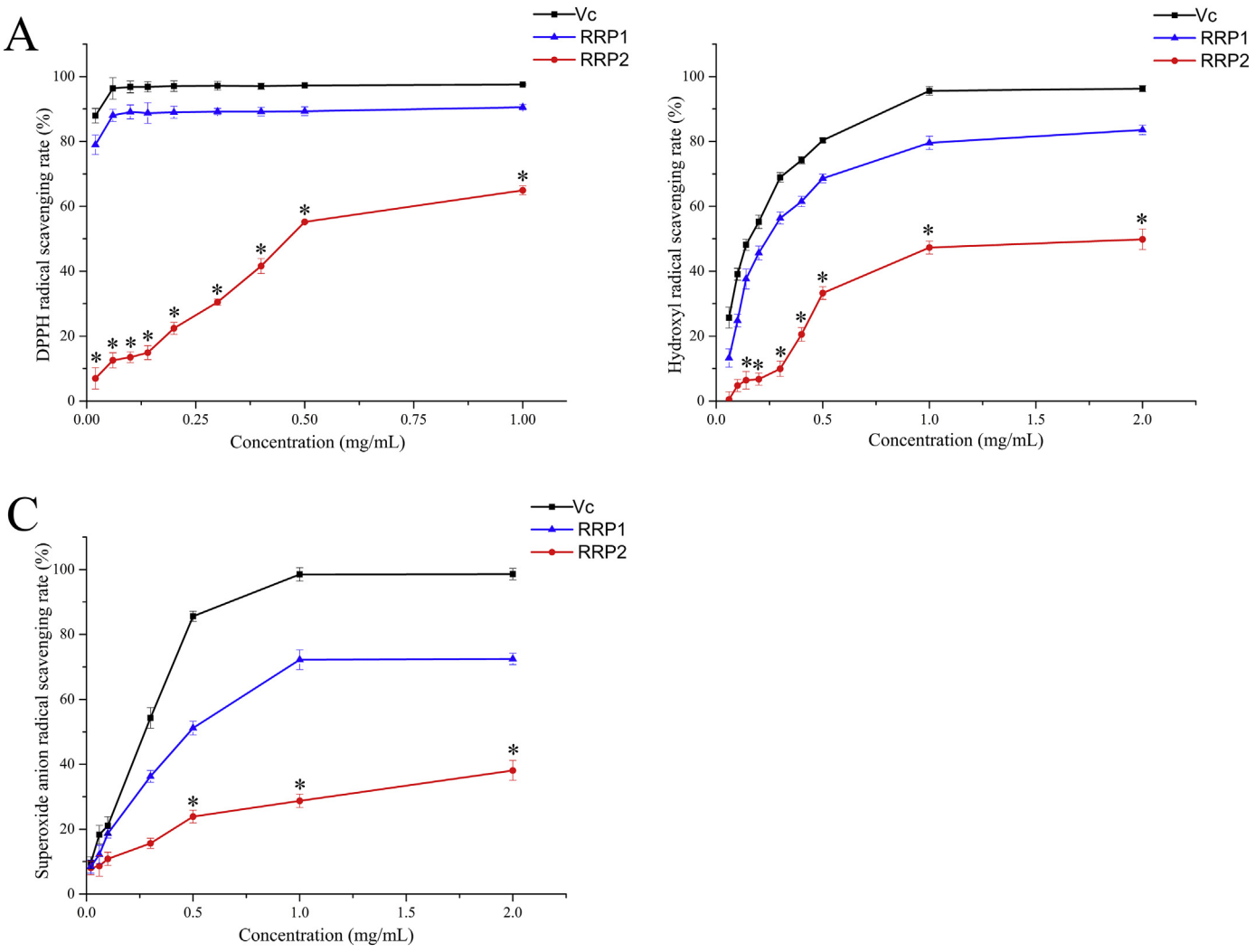

Fig. 4. DPPH radical scavenging activity (A), hydroxyl radical scavenging activity (B) and superoxide radical scavenging activity (C) of RRP1 and RRP2. Values were presented as mean ± SD ($n = 3$). *$P < 0.05$, compared to the RRP1.

shaped" peak at the angle (2θ) about 29° suggesting that RRP2 possessed a more ordered helical structure than RRP1 [28].

3.2.4. Congo red test

The complexation of Congo red with polysaccharides possessing a helical conformation could result in a bathochromic shift of the maximum absorption λ of the complex, in comparison with pure Congo red [28]. As shown in Fig. 3B, compared with Congo red, maximum absorption λ of the Congo red+RRP1 complex showed a distinct bathochromic shift when the concentration of NaOH was increased to 0.1 M, followed by a slow decrease as the NaOH concentration continued to increase, indicating that RRP1 possessed a triple helical conformation. By contrast, the visible absorbance of Congo red+RRP2 complex was similar to that of the pure Congo red which decreased in tandem with the increase of NaOH concentrations, suggesting that the conformation of RRP2 in solution was not triple-helical. The RRP1 and RRP2 possessed significantly different senior structures, which might lead to varying bioactivities.

3.2.5. Scanning electron microscopy (SEM)

In this study, SEM assay was performed to analyze the surface morphology of the polysaccharides [29]. As shown in Fig. 3C, the surface of RRP1 showed a small lamellar or irregular dendritic structure. Fig. 3D showed that RRP2 had a smooth surface topography with characteristic large wrinkles and drop-shaped bulges on the edges. The results

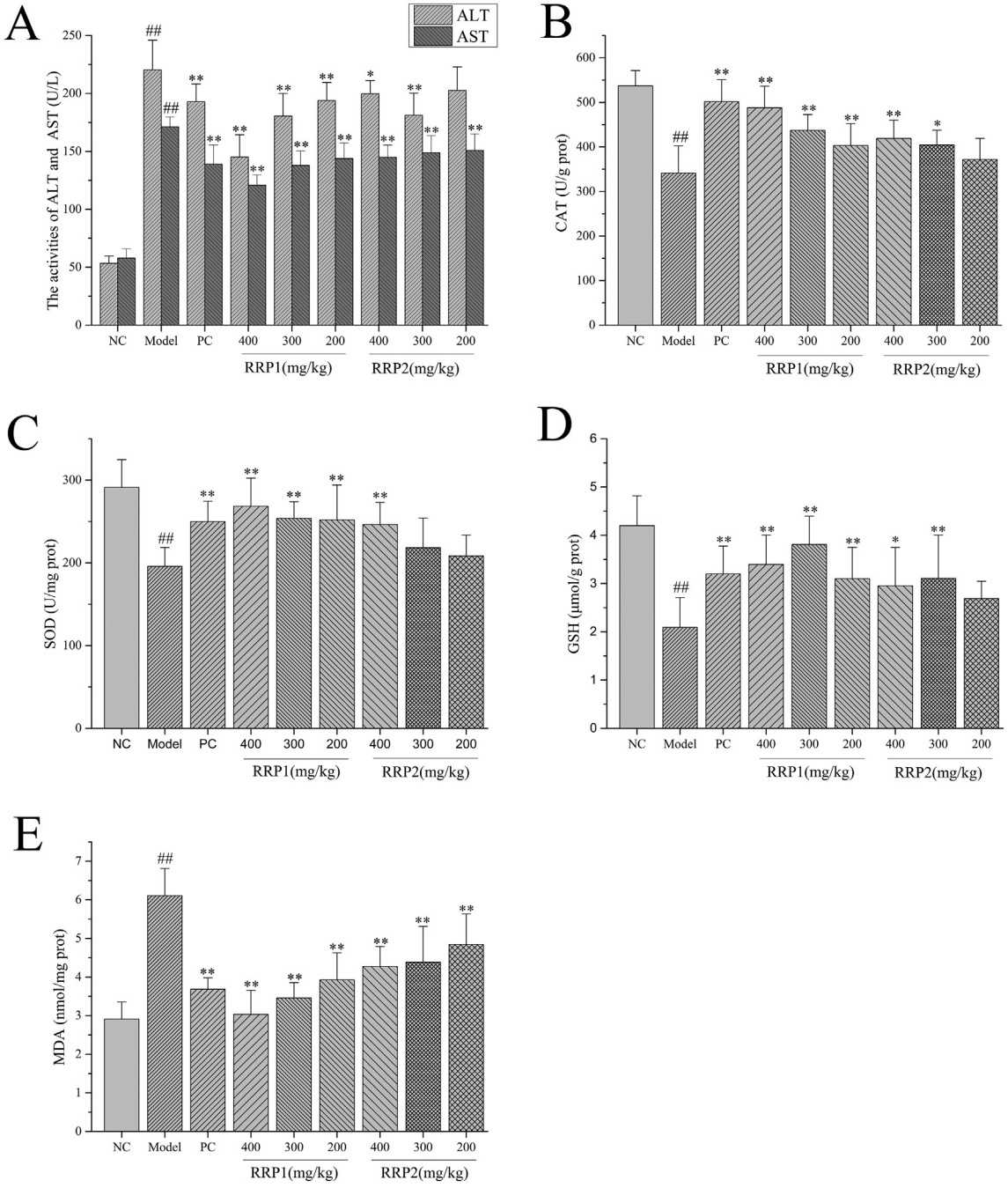

Fig. 5. Effects of RRP1 and RRP2 on serum ALT, AST (A), and hepatic CAT (B), SOD (C), GSH (D) and MDA (E) levels against acute CCl_4-induced liver damage in mice. All values are expressed as means ± SD ($n = 8$). Mice were treated intragastrically with RRP1 and RRP2 (200, 300 and 400 mg/kg bodyweight) or silybin (100 mg/kg bodyweight) once daily for 7 consecutive days prior to the single administration of CCl_4 (2%, intraperitoneally). $^{\#\#}P < 0.01$, compared with the normal control group. $^{*}P < 0.05$, $^{**}P < 0.01$, compared to the model control group.

indicate the differences in morphological properties between RRP1 and RRP2.

3.2.6. Atomic force microscopy (AFM)

AFM is a powerful and visual tool for directly observing the morphological structure at the molecular level [28,30]. As shown in Fig. 3E and G, RRP1 showed irregular island-like structures, suggesting partial aggregation of the polysaccharide chains in RRP1 [12]. Moreover, the height of RRP1 chain structure recorded by AMF ranged from 1 to 3.5 nm, which was higher than that of the single polysaccharide chain (0.1–1 nm) in previous reports [31], indicating that the molecular chains in RRP1 were branched and entangled. By contrast, uniformly-distributed dome/pyramid-like structures with the height ranging from 1 to 4.5 nm were recorded in RRP2 at room temperature (Fig. 3F and H), indicating that RRP2 had branches and no molecular aggregations.

3.3. Antioxidant activities in vitro

In this study, in vitro antioxidant activity of RRP1 and RRP2 was evaluated via assessing the scavenging effects on DPPH radical, hydroxyl (·OH) radical and superoxide radical.

The DPPH radical scavenging determination is a common method that has been widely used to assess the free radical scavenging activity of natural antioxidants [32]. As shown in Fig. 4A, RRP1 displayed slightly weaker scavenging activity than vitamin C (Vc), while RRP2 exhibited a significantly ($P < 0.05$) decreased scavenging ability when compared to both Vc and RRP1. This result indicated that RRP1 possessed a stronger scavenging activity than RRP2 at the various tested concentrations.

·OH is one of the strongest oxidation potential among ROS. Excess amount of free ·OH radicals could damage principal biomolecules such as proteins, lipids, and nucleic acids, which could lead to carcinogenesis, mutagenesis, cytotoxicity and other chronic diseases [33]. Fig. 4B revealed a dose-dependent manner in scavenging the ·OH radical by RRP1, RRP2 and the positive control Vc. However, the faction RRP1 exhibited an excellent scavenging activity that was close to Vc but significantly ($P < 0.05$) stronger than RRP2.

Furthermore, RRP1 and RRP2 showed similar effects on scavenging the superoxide anion free radical to that on the ·OH radical (Fig. 4C). These findings demonstrated that RRP1 had stronger radical scavenging effects than RRP2.

3.4. Hepatoprotective activity in vivo

3.4.1. ALT and AST

The serum ALT and AST levels can reflect the pathological changes in liver. Hepatocytes damage could result in significantly elevated ALT and AST levels [34]. As depicted in Fig. 5A, the serum levels of ALT and AST in CCl_4-induced model mice were remarkably increased ($P < 0.01$) compared to the normal control group, indicating the successful modeling. The animals treated with the *Rhodiola rosea* polysaccharides (both RRP1 and RRP2) showed drastically decreased ALT and AST levels in serum ($P < 0.05$), which was comparable to those treated with the positive control silybin (100 mg/kg). Moreover, RRP1 which showed effects on lowering ALT and AST levels in a dose dependent manner had slightly greater ability to decrease ALT and AST than RRP2. When treated with RRP1 at 400 mg/kg, the lowest ALT and AST levels could be observed in the CCl_4-induced model mice. These data demonstrated that RRP1 and RRP2 had excellent ability in lowering serum ALT and AST levels in the CCl_4-induced model mice.

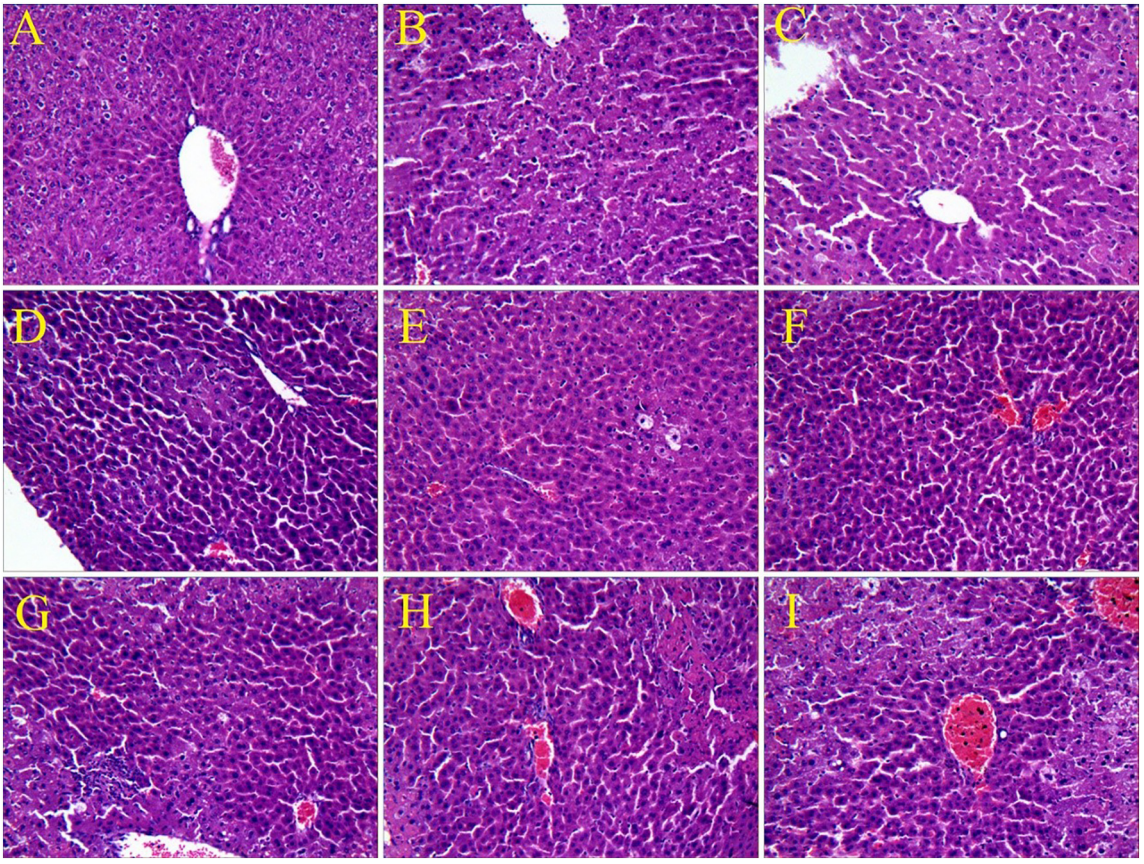

Fig. 6. Histopathological changes in mice livers, stained with H&E (200×). (A) Normal control group, (B) CCl_4-induced model group, (C) Positive control group, (D-F) RRP1 groups at doses of 400, 300, 200 mg/kg, respectively, (G-I) RRP2 groups at 400, 300 and 200 mg/kg, respectively.

3.4.2. CAT, SOD, GSH and MDA

Enzymatic antioxidant defenses including SOD and CAT are involved in direct elimination of ROS. GSH is the most abundant low-molecular weight endogenous antioxidant in maintaining the integrity of cells. MDA reflects the degree of lipid peroxidation [35]. After the treatment with CCl_4, the model mice showed a significantly decreased levels of CAT, SOD, GSH ($P < 0.01$) and markedly increased MDA (Fig. 5B, C, D and E), indicating the CCl_4-induced hepatotoxicity in mice. When treated with the *Rhodiola rosea* polysaccharides (RRP1 and RRP2) with various concentrations, the levels of CAT, SOD and GSH were increased to different degrees, while the content of MDA were significantly decreased ($P < 0.01$) (Fig. 5B, C, D and E). Notably, RRP1 showed generally greater effects than RRP2 on liver protection by increasing the levels of CAT, SOD, GSH and lowering MDA. Moreover, the levels of CAT and SOD increased markedly ($P < 0.01$) (Fig. 5B and C), while the level of MDA decreased significantly ($P < 0.01$) (Fig. 5E), in a dose dependent manner, when treated with RRP1 at various concentrations. Encouragingly, RRP1 at the dose of 400 mg/kg displayed hepatoprotective effects comparable, if not greater, to the positive control silybin. It's interesting that both RRP1 and RRP2 exhibited the highest activity (close to that of silybin) in increasing the GSH level at the concentration of 300 mg/kg (Fig. 5D).

3.4.3. Liver histopathological examination

To further support the evidence of the biochemical analysis, the histopathological changes of livers in each group were illustrated in Fig. 6. In the normal control group (Fig. 6A), the structure of liver lobule was intact with the hepatic cord arranging neatly and regularly. The morphology of liver cells was normal and radiating from central vein to the periphery of the lobules. However, liver lobules of CCl_4 treated mice showed hepatocellular necrosis and the hepatic cord had extensive infiltration of inflammatory cells (Fig. 6B). Compared with that in the model group, the damage of liver cells was significantly alleviated in RRP1 treated groups (Fig. 6D–F): the liver cells became neater and well arranged, the appearance of liver lobule was close to that of the normal control, and less inflammatory infiltration area could be observed. In the positive control group (Fig. 6C) and RRP2 groups (Fig. 6G–I), the hepatic damage ameliorated in different degrees with numbers of the necrotic cells decreased, but there were still some infiltrative inflammatory cells and the loss of cellular boundaries. Hence, the histopathological observation was consistent with the biochemical results.

4. Conclusion

In this study, two different polysaccharide fractions (RRP1 and RRP2) were isolated from rhizome and roots of *Rhodiola rosea*, for the first time, to explore their antioxidant activity in vitro and hepatoprotective effects in vivo. The systematic characterization of two fractions were performed in terms of their molecular weights, monosaccharide composition, and the primary and senior structures. Importantly, the fraction RRP1 had superior antioxidation than RRP2 as indicated by their different scavenging effects on DPPH radical, superoxide radical and hydroxyl radical. Furthermore, the RRP1 fraction exhibited more prominent hepatoprotective prospect than RRP2 against CCl_4 induced liver injury in mice by decreasing ALT and AST levels in serum and MDA in the liver tissue, as well as increasing the levels of CAT, SOD, and GSH the liver tissue homogenates. Taken together, our findings strongly proposed that the polysaccharide fraction RRP1 form the traditional Chinese medicine *Rhodiola rosea* could be developed as a potential therapeutic drug for hepatic disorders.

Declaration of interest

The authors declare no conflicts of interest.

Acknowledgements

This work was supported by National Natural Science Foundation of China (81373371, 81473172, 81503025 and 81773695), National "Twelfth Five-Year" Plan for Science & Technology Support (Grant 2013BAD16B07-1), Special Funds for 331 projects and Industry-University-Research Institution Cooperation (JHB2012-37, GY2010023, GY2011082, GY2012049, GY2013055) in Jiangsu Province and Zhenjiang City, Program for Scientific Research Innovation Team in Colleges and Universities of Jiangsu Province (SJK-2015-4), and a project funded by the Priority Academic Program Development of Jiangsu Higher Education Institutions. The authors also thank the University Ethics Committee for the kind guidance in the animal experiments.

Appendix A. Supplementary data

Supplementary data to this article can be found online at https://doi.org/10.1016/j.ijbiomac.2018.05.168.

References

[1] R. Kandimalla, S. Kalita, B. Saikia, B. Choudhury, Y.P. Singh, K. Kalita, S. Dash, J. Kotoky, Antioxidant and hepatoprotective potentiality of *Randia dumetorum* Lam. leaf and bark via inhibition of oxidative stress and inflammatory cytokines, Front. Pharmacol. 7 (2016).
[2] Y. Feng, C. Sun, Y. Yuan, Z. Yuan, J. Wan, C.K. Firempong, E. Omari-Siaw, X. Yang, Z. Pu, J. Yu, Enhanced oral bioavailability and in vivo antioxidant activity of chlorogenic acid via liposomal formulation, Int. J. Pharm. 501 (1–2) (2016) 342.
[3] M.M. Sayed-Ahmed, A.M. Aleisa, S.S. Al-Rejaie, A.A. Al-Yahya, O.A. Al-Shabanah, M.M. Hafez, M.N. Nagi, Thymoquinone attenuates diethylnitrosamine induction of hepatic carcinogenesis through antioxidant signaling, Oxidative Med. Cell. Longev. 3 (4) (2010) 254–261.
[4] J.K. Yan, Y.Y. Wang, Random-centroid optimization of ultrasound-assisted extraction of polysaccharides from cordyceps sinensis mycelium, Curr. Top. Nutraceutical Res. 13 (4) (2015) 167–171.
[5] J.X. Nan, Y.Z. Jiang, E.J. Park, G. Ko, Y.C. Kim, D.H. Sohn, Protective effect of *Rhodiola sachalinensis* extract on carbon tetrachloride-induced liver injury in rats, J. Ethnopharmacol. 84 (2–3) (2003) 143–148.
[6] M. Dubois, K. Gilles, J.K. Hamilton, P.A. Rebers, F. Smith, A colorimetric method for the determination of sugars, Nature 168 (4265) (1951) 167.
[7] M.M. Bradford, A rapid and sensitive method for the quantitation of microgram quantities of protein utilizing the principle of protein-dye binding, Anal. Biochem. 72 (1976) 248–254.
[8] P. Kumar, V. Kumar, Estimation of uronic acids using diverse approaches and monosaccharide composition of alkali soluble polysaccharide from *Vitex negundo* Linn, Carbohydr. Polym. 165 (2017) 205–212.
[9] W. Deng, M. Fu, Y. Cao, X. Cao, M. Wang, Y. Yang, R. Qu, J. Li, X. Xu, J. Yu, Angelica sinensis polysaccharide nanoparticles as novel non-viral carriers for gene delivery to mesenchymal stem cells, Nanomedicine 9 (8) (2013) 1181–1191.
[10] W. Jia, C. Sun, Z. Yan, H. Pan, Y. Zhou, Y. Fan, The effective mechanism of the polysaccharides from Panax ginseng on chronic fatigue syndrome, Arch. Pharm. Res. 37 (4) (2014) 530–538.
[11] X. Zhang, L. Liu, C. Lin, Isolation, structural characterization and antioxidant activity of a neutral polysaccharide from sisal waste, Food Hydrocoll. 39 (5) (2014) 10–18.
[12] Y. Gao, Y. Zhou, Q. Zhang, K. Zhang, P. Peng, L. Chen, B. Xiao, Hydrothermal extraction, structural characterization, and inhibition HeLa cells proliferation of functional polysaccharides from Chinese tea Zhongcha 108, J. Funct. Foods 39 (2017) 1–8.
[13] C. Chen, B. Zhang, Q. Huang, X. Fu, R.H. Liu, Microwave-assisted extraction of polysaccharides from *Moringa oleifera* Lam. leaves: characterization and hypoglycemic activity, Ind. Crop. Prod. 100 (2017) 1–11.
[14] L. Yang, H. Qu, G. Mao, T. Zhao, L. Fang, B. Zhu, B. Zhang, X. Wu, Optimization of subcritical water extraction of polysaccharides from *Grifola frondosa* using response surface methodology, Pharmacogn. Mag. 9 (34) (2013) 120.
[15] L. Liang, X. Wu, M. Zhu, W. Zhao, F. Li, Y. Zou, L. Yang, Chemical composition, nutritional value, and antioxidant activities of eight mulberry cultivars from China, Pharmacogn. Mag. 8 (31) (2012) 215.
[16] L.C. Peng, H. Li, Y.H. Meng, Layer-by-layer structured polysaccharides-based multilayers on cellulose acetate membrane: towards better hemocompatibility, antibacterial and antioxidant activities, Appl. Surf. Sci. 401 (2017) 25–39.
[17] T. Zhao, Y. Fan, G. Mao, W. Feng, Y. Zou, Y. Zou, L. Yang, X. Wu, Purification, characterization and antioxidant activities of enzymolysis polysaccharide from *Grifola frondosa*, Iran. J. Pharmacol. Res. 16 (1) (2017) 347–356.
[18] C.H. Su, M.N. Lai, L.T. Ng, Effects of different extraction temperatures on the physicochemical properties of bioactive polysaccharides from *Grifola frondosa*, Food Chem. 220 (2017) 400–405.
[19] C. Li, Q. Huang, X. Fu, X.J. Yue, R.H. Liu, L.J. You, Characterization, antioxidant and immunomodulatory activities of polysaccharides from *Prunella vulgaris* Linn, Int. J. Biol. Macromol. 75 (2015) 298–305.

[20] T. Zhao, G. Mao, R. Mao, Y. Zou, D. Zheng, W. Feng, Y. Ren, W. Wang, W. Zheng, J. Song, Antitumor and immunomodulatory activity of a water-soluble low molecular weight polysaccharide from *Schisandra chinensis* (Turcz.) Baill, Food Chem. Toxicol. 55 (3) (2013) 609–616.
[21] X. Li, B. Zhang, J. Li, J. Zhou, X. He, L. Ye, J. Zou, C. Wu, X. Zhang, W. Peng, Purification, characterization, and complement fixation activity of acidic polysaccharides from *Tuber sinoaestivum*, LWT- Food Sci. Technol. 85 (2017).
[22] E.G. Shakhmatov, V.A. Belyy, E.N. Makarova, Structural characteristics of water-soluble polysaccharides from Norway spruce (*Picea abies*), Carbohydr. Polym. 175 (2017) 699.
[23] Y. Chai, M. Zhao, Purification, characterization and anti-proliferation activities of polysaccharides extracted from *Viscum coloratum* (Kom.) Nakai, Carbohydr. Polym. 149 (2016) 121–130.
[24] Q.L. Luo, Z.H. Tang, X.F. Zhang, Y.H. Zhong, S.Z. Yao, L.S. Wang, C.W. Lin, X. Luo, Chemical properties and antioxidant activity of a water-soluble polysaccharide from *Dendrobium officinale*, Int. J. Biol. Macromol. 89 (2016) 219.
[25] J. Jiang, F. Kong, N. Li, D. Zhang, C. Yan, H. Lv, Purification, structural characterization and in vitro antioxidant activity of a novel polysaccharide from Boshuzhi, Carbohydr. Polym. 147 (2016) 365.
[26] K.B. Jeddou, F. Chaari, S. Maktouf, O. Nouri-Ellouz, C.B. Helbert, R.E. Ghorbel, Structural, functional, and antioxidant properties of water-soluble polysaccharides from potatoes peels, Food Chem. 205 (Supplement C) (2016) 97–105.
[27] X. Li, L. Wang, Z. Wang, Structural characterization and antioxidant activity of polysaccharide from *Hohenbuehelia serotina*, Int. J. Biol. Macromol. 98 (2017) 59–66.
[28] W. Kai-Ping, J. Wang, L.I. Qiang, Z. Qi-Lin, Y. Ru-Xu, Y. Cheng, L.I. Luo, Y.U. Zhang, Structural differences and conformational characterization of five bioactive polysaccharides from *Lentinus Edodes*, Food Res. Int. 62 (8) (2014) 223–232.
[29] X.C. Liu, Z.Y. Zhu, Y.L. Tang, M.F. Wang, Z. Wang, A.J. Liu, Y.M. Zhang, Structural properties of polysaccharides from cultivated fruit bodies and mycelium of *Cordyceps militaris*, Carbohydr. Polym. 142 (2016) 63–72.
[30] Y. Gao, Y. Zhou, Q. Zhang, K. Zhang, P. Peng, L. Chen, B. Xiao, Hydrothermal extraction, structural characterization, and inhibition HeLa cells proliferation of functional polysaccharides from Chinese tea Zhongcha 108, J. Funct. Foods 39 (Supplement C) (2017) 1–8.
[31] L. Wang, H.M. Liu, G.Y. Qin, Structure characterization and antioxidant activity of polysaccharides from Chinese quince seed meal, Food Chem. 234 (2017) 314.
[32] B. Ren, C. Chen, C. Li, X. Fu, L. You, R.H. Liu, Optimization of microwave-assisted extraction of *Sargassum thunbergii* polysaccharides and its antioxidant and hypoglycemic activities, Carbohydr. Polym. 173 (2017) 192–201.
[33] T. Sakai, J. Imai, T. Ito, H. Takagaki, M. Ui, S. Hatta, The novel antioxidant TA293 reveals the role of cytoplasmic hydroxyl radicals in oxidative stress-induced senescence and inflammation, Biochem. Biophys. Res. Commun. 482 (4) (2017) 1183–1189.
[34] X.B. Yang, S. Yang, Y.R. Guo, Y.D. Jiao, Y. Zhao, Compositional characterisation of soluble apple polysaccharides, and their antioxidant and hepatoprotective effects on acute CCl4-caused liver damage in mice, Food Chem. 138 (2–3) (2013) 1256–1264.
[35] M.Z. Jiang, In Vitro and In Vivo Studies of Antioxidant Activities of Flavonoids From *Adiantum capillus-veneris* L, 2011.